MIXED-MODE COHESIVE-ZONE MODELS FOR DELAMINATION AND DEFLECTION IN COMPOSITES

M. D. Thouless* and J. P. Parmigiani**

* Department of Mechanical Engineering,
Department of Materials Science & Engineering,
University of Michigan, Ann Arbor, MI 48109, USA.
** Department of Mechanical Engineering
Oregon State University, Corvallis, OR 97331, USA.

ABSTRACT

Cohesive-zone models for interfaces incorporate both strength and energy parameters. Therefore, they provide a natural bridge between strength-based models and energy-based models for fracture, allowing delamination to be described by a single framework that covers a range of applications for which the strength or energy criteria alone might not be sufficient. In this paper, the relationships between cohesive-zone models and fracture models based on strength or energy are discussed. A mixed-mode formulation of cohesive-zone models has been used to investigate a number of issues related to the delamination of interfaces. It has been shown that linear-elastic fracture mechanics (LEFM) provides an excellent description of mixed-mode delamination, beyond the limits where LEFM would usually be thought to be appropriate. In particular, the concept of a nominal phase angle, calculated from stress-intensity factors is very robust. Compressive normal stresses on interfaces can be accommodated by the finite thickness of cohesive-zone models, resulting in increased levels of nominal toughness. The length scale naturally associated with cohesive zones allows them to describe mixed-mode fracture of interfaces with a modulus mismatch across them. Cohesive-zone models have also been used to explore the phenomenon of crack deflection at interfaces. The results of these calculations appear to be more consistent with strength-based models of deflection, rather than with energy-based models. They indicate that the strength ratio between the cohesive strengths of the interface and substrate play an important role in determining whether crack deflection or propagation occurs.

1. INTRODUCTION

Crack propagation along interfaces often controls the mechanical behaviour of composites (Fig. 1). The toughness of a fibre composite depends on delamination of the matrix-fibre interfaces, and frictional sliding along the interfaces. Failure of laminated composites can

occur by delamination of the plies. However, crack deflection along interfaces, and multiple delaminations between successive plies or bonded interfaces, can lead to enhanced tensile strengths and energy dissipation. Historically, two approaches have been used to analyze these aspects of composite mechanics: a strength-based approach to fracture (Inglis 1913), and an energy-based approach (Griffith 1920). While the energy-based approach of fracture mechanics is the most versatile of the two for linear-elastic systems, and is the dominant tool currently used for analysis, there are regimes for which the other approach may be more appropriate (particularly at small length scales). Furthermore, for many practical applications, such as when large-scale plasticity dominates the fracture process, neither approach is sufficient. The relatively recent development of numerical cohesive-zone analyses provides a much more general model of fracture and allows the limiting regimes, in which either energy or strength alone are the dominant failure criteria, to be bridged within a single framework.

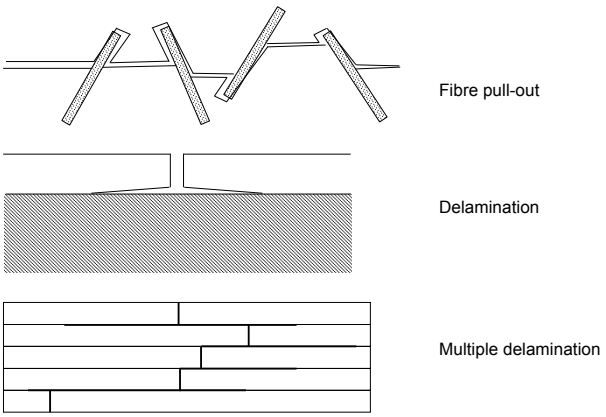

Fig. 1: Effects of interfacial failure and crack deflection in composites. Figure adapted from Parmigiani and Thouless (2006).

2. MODELS OF FRACTURE

2.1 Energy-based approach to fracture. The energy-based approach to fracture assumes that crack growth occurs when the energy-release rate $\mathcal{G}$ reaches a critical value, Γ, the toughness. However, when delamination of an interface occurs, the crack is constrained by geometry to grow along a fixed path. Depending on the geometry and the nature of the applied loads, the crack may grow under mixed-mode conditions with both normal and shear components to the crack-tip deformation, and the toughness of an interface is a function of the relative amounts of normal and shear deformation. Experimental observations indicate that the toughness under pure mode-II conditions, Γ_{II}, is generally larger than the toughness under pure mode-I conditions, Γ_I. The relative proportions of shear to normal deformations contributing to crack growth is defined by interfacial fracture mechanics through use of a concept known as the phase angle. In a plane problem, and in the absence of a modulus mismatch across the interface, the nominal phase angle, ψ^∞, is defined in terms of the nominal mode-II and mode-I stress intensity factors, K_I and K_{II} as calculated from the assumption

of sharp cracks and linear elasticity:

$$\psi^{\infty} = \tan^{-1}\left(K_{II}/K_{I}\right). \tag{1}$$

This can be re-expressed in terms of the mode-I and mode-II energy-release rate components, $\mathcal{G}_I$ and $\mathcal{G}_{II}$ as

$$\psi^{\infty} = \tan^{-1}(\sqrt{\mathcal{G}_{II}/\mathcal{G}_{I}}), \tag{2}$$

where the total energy-release rate is the sum of the two components:

$$\mathcal{G} = \mathcal{G}_I + \mathcal{G}_{II}. \tag{3}$$

A mixed-mode failure criterion is established by assuming that the toughness is a function of the nominal phase angle, so that it varies from Γ_I when $\psi^{\infty} = 0^o$ to Γ_{II} when $\psi^{\infty} = 90^o$. Many different functional dependences have been proposed in the literature; they are generally monotonic between the two limits and, beyond the observation that the effects of mode-II can often be neglected at phase angles below about 45^o, experimental observations tend not to be sensitive enough to argue for one particular function over another. One functional dependence, that follows the general trend of experimental observations, results from an assumption that the values of the two components of the energy-release rate at fracture are given by the condition:

$$\frac{\mathcal{G}_I}{\Gamma_I} + \frac{\mathcal{G}_{II}}{\Gamma_{II}} = 1. \tag{4}$$

If these components are denoted by ${\mathcal{G}_I}^*$ and ${\mathcal{G}_{II}}^*$, so that

$$\frac{{\mathcal{G}_I}^*}{\Gamma_I} + \frac{{\mathcal{G}_{II}}^*}{\Gamma_{II}} = 1, \tag{5}$$

then the mixed-mode toughness of the interface is given by

$$\Gamma = {\mathcal{G}_I}^* + {\mathcal{G}_{II}}^*, \tag{6}$$

at a phase angle of

$$\psi^{\infty} = \tan^{-1}\left(\sqrt{{\mathcal{G}_{II}}^*/{\mathcal{G}_I}^*}\right), \tag{7}$$

Combining Eqns. 5, 6 and 7, results in a mixed-mode failure criterion of

$$\Gamma = \Gamma_I \frac{\lambda(1+\tan^2\psi^{\infty})}{\lambda+\tan^2\psi^{\infty}}, \tag{8}$$

where $\lambda = \Gamma_{II}/\Gamma_I$. This relationship is plotted in Fig. 2. This functional form (or any other similar form) can be used in linear-elastic fracture mechanics (LEFM) analyses to

predict the strength of mixed-mode geometries. The concept of mixed-mode fracture can

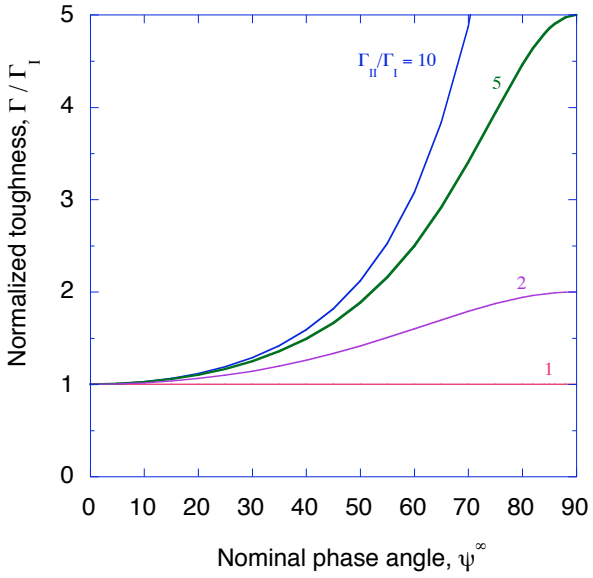

Fig. 2: Dependence of toughness on nominal phase angle following the mixed-mode failure criterion of Eqns. 4 and 8.

be slightly more involved when there is modulus mismatch across the interface. In a plane geometry containing an interface between two different isotropic materials with moduli E_1 and E_2, and Poisson's ratios ν_1 and ν_2, the mechanics depends on two non-dimensional groups of the elastic parameters. These two groups are given by (Dundurs 1969)

$$\alpha = \frac{\bar{E}_1 - \bar{E}_2}{\bar{E}_1 + \bar{E}_2}, \tag{9}$$

and

$$\beta = \frac{\bar{E}_1 f(\nu_2) - \bar{E}_2 f(\nu_1)}{\bar{E}_1 + \bar{E}_2}, \tag{10}$$

where $\bar{E} = E(1-\nu^2)$ and $f(\nu) = (1-2\nu)/[2(1-\nu)]$ in plane strain, and $\bar{E} = E$ and $f(\nu) = (1-2\nu)/2$ in plane stress. If $\beta = 0$, then the discussion of the previous paragraph about mixed-mode fracture still applies, since the shear and normal components of the crack-tip stress field are well-defined. However, if $\beta \neq 0$, the nominal phase angle has to be defined with respect to a characteristic length scale, such as the layer thickness, h_1:

$$\psi^\infty = \tan^{-1}\left[\Re(Kh^{i\epsilon})/\Im(Kh^{i\epsilon})\right], \tag{11}$$

where K is the complex stress-intensity factor (Rice 1988), and

$$\epsilon = (1/2\pi)\ln\left[(1-\beta)/(1+\beta)\right]. \tag{12}$$

Now, the mixed-mode failure criterion depends on the choice of the characteristic length scale chosen to define the phase angle.

The condition for whether a crack impinging on an interface will continue into the underlying substrate, or whether it will deflect along the interface, is computed by comparing the energy-release rate and toughness for two separate problems (He and Hutchinson 1989): (i) for a small kink extending ahead of the crack across the interface, and (ii) for a small kink extending from the crack along the interface (Fig. 3). For a homogeneous composite that has the same modulus on both sides of the interface, crack deflection will occur if the toughness of the interface Γ is less than about 25% of the mode-I toughness of the substrate Γ_2 (He and Hutchinson, 1989; Thouless, Cao and Mataga 1989). However, since the interface is generally under mixed-mode conditions, the ratio of Γ_{II}/Γ_I for the interface also affects the conditions for crack deflection. In particular, the effect of Γ_{II} becomes increasingly important when the crack is trying to penetrate into a compliant material (He and Hucthinson, 1989; He, Evans and Hutchinson, 1994), and crack deflection tends to be suppressed if the interface has a high value of the mode-II toughness.

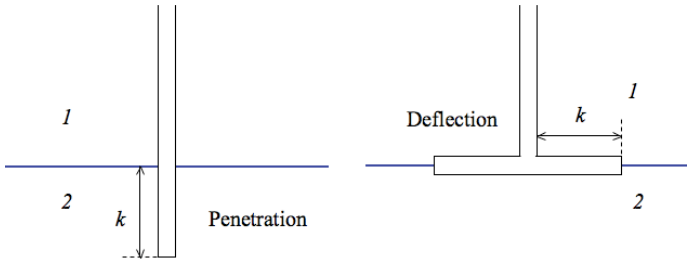

Fig. 3: Crack deflection and crack penetration across an interface are analyzed by considering two distinct geometries: (i) a kink extending across an interface, and (ii) a kink extending along an interface.

2.2 Strength-based approach to fracture. There are two types of strength-based analyses. One type involves elastic stress calculations, with an assumption that an interface fails when the stress reaches a critical value. For example, the normal stress distribution along the interface of a fiber or a laminate being subjected to an applied load (Fig. 4) can be calculated if the stresses are completely elastic along the interface (Muki and Sternberg, 1970). When the maximum stress on the interface reaches a critical value, corresponding to either the normal or shear cohesive strength of the interface, $\hat{\sigma}$ or $\hat{\tau}$, debonding is initiated (Hsueh 1990). While such an elastic calculation gives a value for the debond strength of a fiber or laminate, it is very sensitive to stress concentrations and elastic singularities.

An elastic stress analysis can also be used to compute the conditions for crack deflection at an interface in a composite. A classic example is the Cook-Gordon analysis (Cook and Gordon 1964) in which the normal stresses ahead of a matrix crack (modelled as an elliptical flaw) is compared to the normal stresses along an interface perpendicular to the crack (Fig. 5). By equating the ratio of the maximum values of the two stresses, it can be shown that the debond strength of the interface will be reached before before the matrix crack grows if the cohesive strength of the interface is less than about 20% of the matrix strength. A similar result was also obtained by an elastic stress analysis for cracks approaching an interface with a modulus mismatch (Gupta, Argon and Suo 1992).

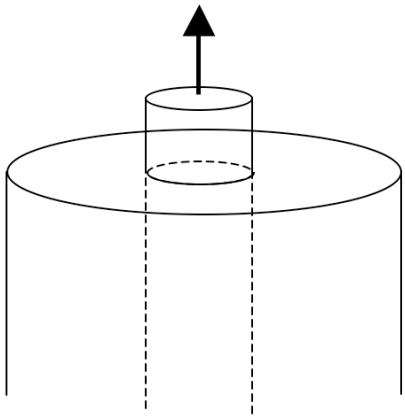

Fig. 4: Stress analysis for debonding of a fibre in a composite.

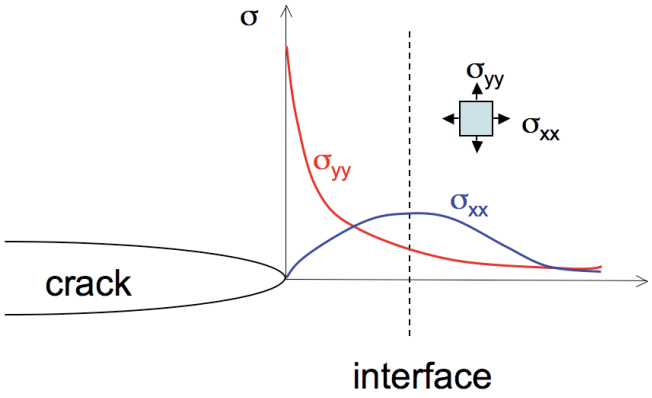

Fig. 5: The Cook-Gordon model for delamination at an interface in a composite.

An alternative type of stress analysis for debonding of an interface, that is less sensitive to the effects for stress concentrations, are shear-lag analyses. In these calculations, it is recognized that the maximum stress that can be supported by an interface is limited by the shear cohesive strength $\hat{\tau}$. But, it is assumed that when this stress level is reached, the interface maintains its stress-bearing capability, with relative slip occurring across the interface. A force equilibrium calculation then permits a calculation of the slip length over which the maximum shear strength is exhbited. For example, if a fibre of radius R is subjected to an applied load P (Fig. 6), then the slip length is $L_c = P/2\pi R\hat{\tau}$.

Embedded within this model is an implicit assumption that an infinite shear strain can be supported across the interface. As the applied load supported by the fibre is increased, it is assumed that the slip length can increase without limit until the fracture strength of the fibre is reached (or until the slip zone extends across the matrix and the fiber is pulled out of the matrix). If there is a limit to the relative displacement that could be accommodated across the interface while still maintaining the full strength of the interface, then the concept of an interfacial toughness would be introduced into such a model. The notion that the properties of an interface can be described by both a strength and a toughness leads naturally into the concept of a cohesive-zone model.

2.3 Cohesive-zone approach to fracture. The toughness of an material or interface is performance limiting for energy-based fracture criteria, but the strength is not. Conversely,

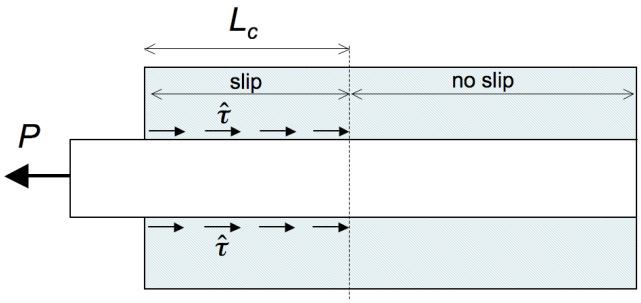

Fig. 6: Shear-lag analysis for a fibre embedded in a matrix.

strength, not toughness, is performance limiting for strength-based fracture criteria. By explicitly modelling the tractions across an interface, cohesive-zone models allow for a full description of fracture that incorporates both types of behaviour. These tractions may be associated with physical, chemical or mechanical bonding across a plane, or they can be associated with the deformation of an intermediate layer between two planes. There is a degree of arbitrariness as to the volume of material assigned to the cohesive-zone, which depends upon the scale at which the fracture process is being described. For example, various amounts of the plastic deformation that may be intimately coupled with crack growth can be incorporated into a cohesive zone. At the most fundamental level, the cohesive zone might incorporate only atom-to-atom bonding, with no plasticity. Less computationally intensive zones will generally include material in which plasticity might occur. The choice of how much plasticity to assign to the fracture process, and how much to assign to the bulk deformation of the material, will depend on what gives an adequate description of failure at the scale of interest within the set of parameters required to describe the problem. For adhesively-bonded joints or laminated composites, a natural size-scale for the cohesive-zone is the thickness of the adhesive layer (Yang, Thouless and Ward 1999; Yang and Thouless 2001) or the interlaminar region. In this case, the properties of the traction-separation law represent the entire deformation of the adhesive layer, and may depend on the details of the geometry. However, this is not an issue limited to cohesive-zone models; energy and strength-based approaches to adhesive fracture all incorporate the same assumption that the entire adhesive layer is associated with the fracture process, and have the same issues of geometry dependence.

In fibre-composite materials, cohesive-zone models can be used to represent the bridging tractions imposed by the pull-out of fibres; the size and properties of the cohesive-zone then have to capture fibre pull-out (Fig. 7). It is possible to use such a traction-separation law to explore the behavior of a tensile composite bar of width, W, with different sizes of initial crack, a_o, (Li, Thouless, Waas, Schrœder and Zavattieri 2005b). A comparison between the predictions for the load-displacement curves and the actual experimental observations are shown in Fig. 8a. It will be observed from this plot that the energy dissipated by the specimen varies with initial crack size. This is related to the stability of the crack (Fig. 8b), and is a geometrical effect captured by the cohesive-zone model, rather than being associated with any change in the cohesive properties.

For complete fidelity in mimicking the fracture process, the traction-separation law of the cohesive should accurately represent the bonding across the interface or the deformation of the bonding layer. In linear-elastic systems this can be determined by a J-integral approach (Li , Maalej and Hashida 1994; Sørenson and Jacobson 2003). However, in general, much of the fracture behavior at a practical engineering scale of observation can be captured

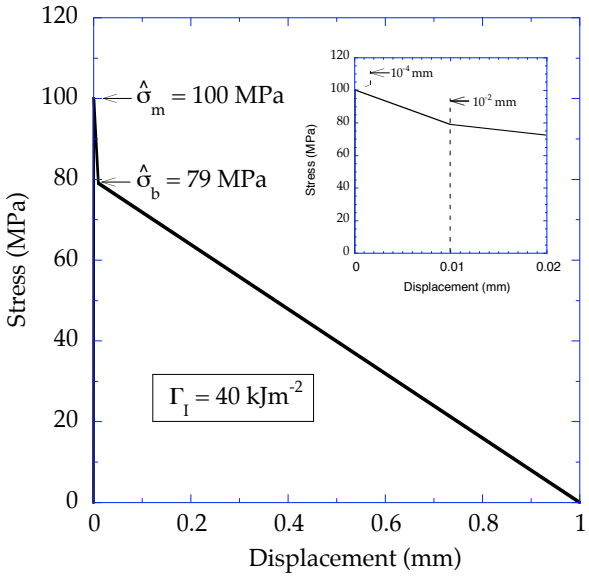

Fig. 7: Traction-separation law for a polymer-matrix composite, with a matrix cracking strength of $\hat{\sigma}_m = 100$ MPa, and a bridging strength of $\hat{\sigma}_b = 79$ MPa. The decreasing portion on the right of the traction-separation law corresponds to fibre pullout, after matrix cracking has occurred. Figure taken from Li, *et al.* (2005a).

by two parameters that describe the cohesive law: the area under the traction-separation curve (the toughness), and a characteristic strength (typically, the cohesive strength) or a characteristic displacement that represents the failure strain of the cohesive zone. Beyond these two parameters, the details of the cohesive law are often not significant for practical purposes.

Mixed-mode fracture can be accommodated within a cohesive-zone model if it is recognized that each mode of the energy-release rate can be defined as the area traversed under the appropriate traction-separation law, as shown in Fig. 9 (Yang and Thouless, 2001). The phase angle can be described at any point along the fracture plane, at all stages during the loading process, by comparing the appropriate ratio of the components of the energy-release rate:

$$\psi = \tan^{-1}\left[\frac{\mathcal{G}_{II}}{\mathcal{G}_I}\right]. \tag{13}$$

Of particular interest is the energy-release rate at the tip of the crack, just when the crack is about to advance. This is given by

$$\psi_o = \tan^{-1}\left[\frac{\mathcal{G}^*_{II}}{\mathcal{G}^*_I}\right], \tag{14}$$

where $\mathcal{G}^*_{II}$ and $\mathcal{G}^*_I$ are the values of the energy-release rate components at the crack tip that satisfy Eqn. 4. As discussed above (Eqn 6), the sum of these two components (or three components if a mode-III problem is being considered) is equal to the toughness at

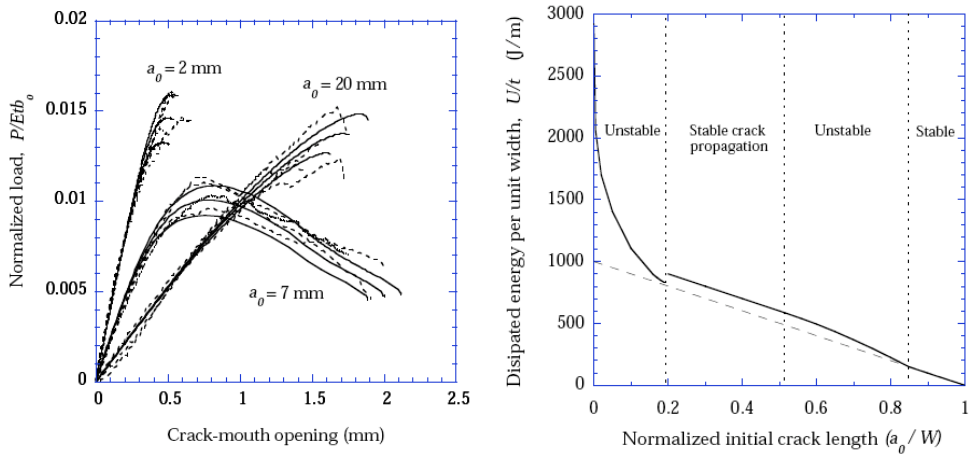

Fig. 8: **(a)** Comparison between load-displacement plot for a tensile specimen of width 25 mm, thickness 2.8 mm, and length 140 mm (gauge length of 25 mm), for different initial crack sizes. **(b)** Energy dissipation as a function of crack length, showing different regimes of stability predicted by the cohesive-zone model. Figures taken from Li, *et al.* (2005b).

the corresponding value of phase angle. In this formulation of mixed-mode fracture, no assumptions need to be made about the nature of the crack tip, and the definitions apply through any arbitrary range of cohesive laws. The same formulation would be applicable for different choices of mixed-mode failure criterion, or cohesive-laws.

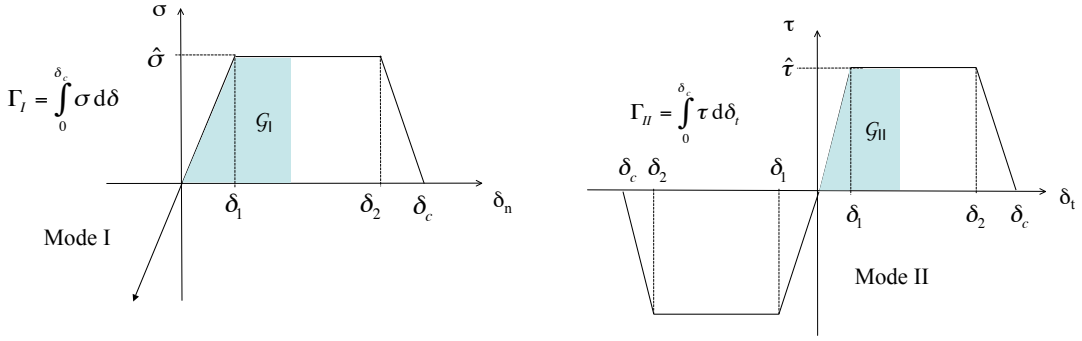

Fig. 9: Traction separation laws for mode-I and mode-II deformation, showing the definitions of the mode-I and mode-II components of the energy-release rate. Figures adapted from Yang and Thouless (2001).

A comparison between the predictions of the mixed-mode cohesive-zone model and the equivalent linear-elastic fracture-mechanics (LEFM) predictions were explored using a simple centrally-cracked bar of modulus $\bar{E}$ with a normal and shear force, P and Q applied to the crack (Parmigiani and Thouless, 2007). Cohesive elements with a traction-separation law of the form shown in Fig. 9 were placed along the entire length of the interface. The elements were *not* embedded in any continuum elastic elements. The LEFM prediction for the failure load, P_{LEFM}, was computed using the form of the mixed-mode failure criterion given

by Eqn. 8. Figure 10a shows how the load for failure, P_f tends to P_{LEFM} at small values of the fracture-length scale (defined as $\bar{E}\Gamma_I/\hat{\sigma}^2$), when the toughness criterion dominates over the strength criterion. The corresponding normal stresses ahead of the crack is shown in Fig. 10b, where an approximation to the expected $1/\sqrt{r}$ stress field can be seen in the limits where LEFM conditions apply. For large values of the fracture-length scale, the stress is uniform across the uncracked ligaments, as would be expected when a strength-criterion for fracture is appropriate.

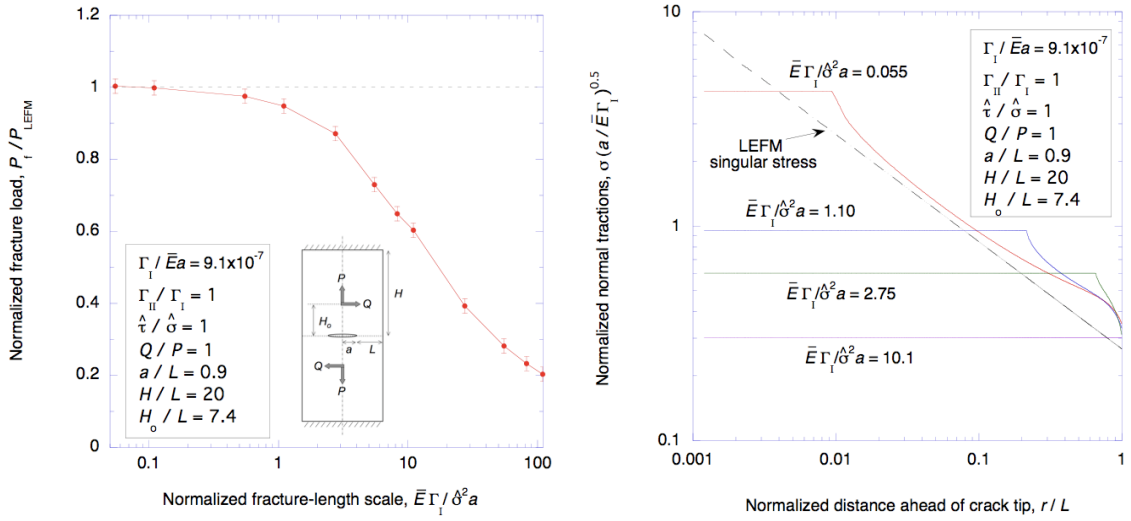

Fig. 10: **(a)** Failure load for a mixed-mode tensile test. **(b)** Normal stresses ahead of a crack in a mixed-mode tensile test. Figures taken from Parmigiani and Thouless (2007).

3. DELAMINATION OF INTERFACES

Any arbitrary loading on a laminated structure can be decomposed into four sets of load acting on an interface crack (Fig. 11): a set of axial forces, N; a set of moments, M; and two sets of shear forces, V_s and V_u. Results from linear-elastic fracture mechanics (LEFM) can be used to compute the combined energy-release rate and nominal phase angle from this complete set of four loads (Suo and Hutchinson, 1990; Li, Wang and Thouless 2004). When combined with a mixed-mode failure criterion such as Eqn. 8, the delamination strength can be computed. In principle, it would be expected that these LEFM results should be accurate in the limit when the stresses at the crack tip are controlled by a $1/\sqrt{r}$ stress field. In the recent work of Parmigiani and Thouless (2007), the LEFM predictions for the phase angle and delamination loads were compared to the results obtained using a cohesive-zone model, to explore the regimes in which the LEFM equations can be used to describe fracture.

3.1 Mixed-mode delamination. Figure 12a shows how the phase angle, as defined from a cohesive-zone calculation (Eqn. 13), varies with distance from the crack tip for a laminated geometry with equal moduli across the interface. As can be seen in that plot, the phase angle asymptotes to a constant value in the region near the crack tip. This constant value is equal to ψ^∞, the value based on LEFM predictions. While it is the phase angle at the crack tip, ψ_o, that controls fracture, Fig. 12a shows there is nothing special about the crack tip. This would be consistent with a constant value of the phase angle expected in the

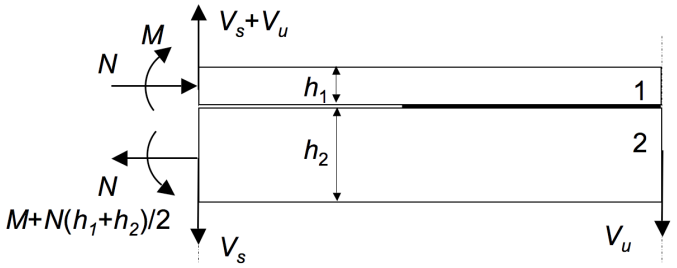

Fig. 11: Any arbitrary loading on a laminated structure can be decomposed into four sets of load acting on an interface crack: a set of axial forces, N; a set of moments, M; and two sets of shear forces, V_s and V_u.

immediate vicinity of a crack tip where the stresses are dominated by the singular stress field in an a linear-elastic geometry. However, a plot of the normal and shear stresses along the interface (Fig 12b) shows that there is nothing remotely resembling a $1/\sqrt{r}$ stress field for this particular set of cohesive properties. Furthermore, the phase angle matches ψ^∞ in the region where the stresses are limited by the cohesive strengths.* LEFM calculations provide accurate predictions of the phase angle and, hence, of the strength of elastic laminated geometries, even when the actual fracture-length scales of the interface are far in excess of what might have been expected to approximate LEFM conditions. An example of the range of fracture length scales over which LEFM calculations appear to provide reasonably accurate predictions for the strength are shown in Fig. 13a. In this context it should be noted that when the toughness does not depend on phase angle, the energy-release rate associated with the moment and axial components of the loading on the crack tip do not depend on the nature of the interface, only the shear component is affected (Li, *et al.* 2004). For this reason, the results for $\Gamma_{II}/\Gamma_I = 1$ tend to be particularly accurate even for very large fracture length scales. The accuracy of the phase angle for this particular mixed-mode geometry, which is more dominated by mode-II than the geometry shown in Fig 12, is illustrated in Fig 13b.

3.2 Effects of crack-tip compression. One issue into which a cohesive-zone model gives particular insight is fracture under conditions when the crack tip is subjected to a closing normal force. Experimentally, fracture is seen under these conditions (Thouless, Liniger and Hutchinson 1992; Thouless, Liniger and Jensen 1994), but the concept of a negative mode-I is generally rejected owing to the implication of crack-surface interpenetration. For LEFM analyses, it is assumed that crack-surface contact enforces conditions of pure mode-II on the crack tip, with the possibility of additional energy dissipation associated with friction (Stringfellow and Freund 1992). However, the effects of friction do not seem to be great enough to account for the rise in fracture resistance above the mode-II toughness that can be seen (Thouless *et al.* 1992).

A cohesive-zone approach to fracture introduces the concept that all fracture planes (especially, laminates and joints with a compliant adhesive layer) have a non-zero value of equilibrium thickness, and can accommodate some normal compression. This normal compression can store energy, beyond that associated with frictional effects, but will not contribute to failure, which is expected to occur when $\mathcal{G}_{II} = \Gamma_{II}$. If the interface is very thin, the contri-

*In this regard, it is noted that a definition of phase angle based on shear-to-normal stress ratios, as the phase angle is sometimes described in terms of, would fail in a cohesive-zone context, because it would just give the ratio of the two cohesive strengths.

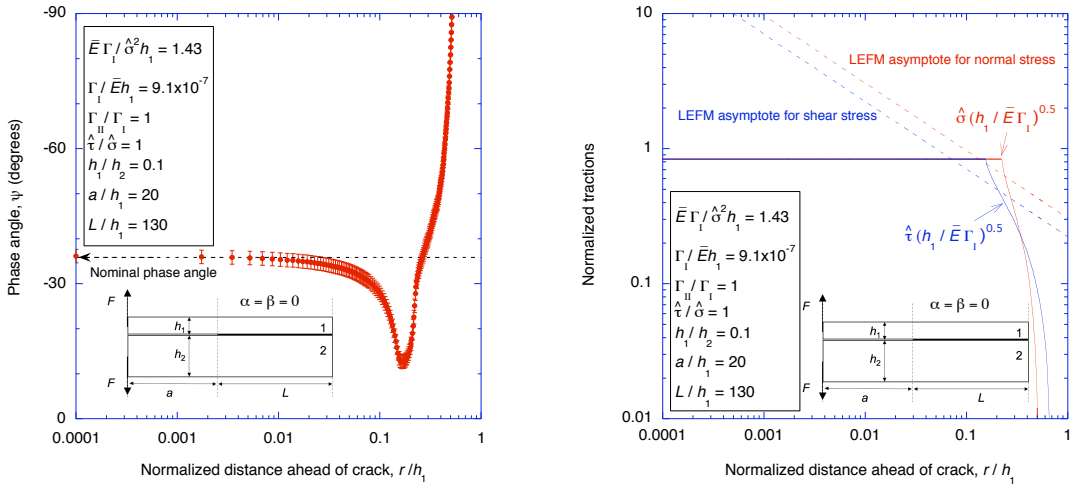

Fig. 12: **(a)** Variation of phase angle with distance from crack tip in a cohesive-zone model **(b)** Normal and shear stresses ahead of a crack. Figures adapted from Parmigiani and Thouless (2007).

bution of the mode-I compression will be minimal. However, if the interface is thicker, the mode-I compression can be more significant. This is demonstrated in Fig. 14. The load to fracture a laminated geometry calculated from a cohesive-zone model was used to compute a nominal toughness using the equations of linear-elasticity. The nominal phase angle was changed by varying the ratio of the axial to transverse load, and the loading conditions were taken over a range for which LEFM would predict a compressive normal stress on the interface (corresponding to nominal phase angles with a magnitude greater than 90^o). The resultant plots of nominal toughness against nominal phase angle (both calculated from the geometry and loads using LEFM calculations) are shown in Fig. 14 for three conditions: (i) a thin interface with a thickness given by $t = 0.00174h_1$, and no friction between the crack surfaces; (ii) the same interface, but with a coefficient of friction $\mu = 0.5$; (iii) an interface ten times as thick, but with no friction. When the cohesive layer is very thin, the toughness has a maximum value equal to Γ_{II} if there is no frictional dissipation. Friction increases the energy dissipated by fracture (and, hence, the nominal value of toughness). When the thickness of the cohesive zone is large enough, energy can be stored by mode-I compression, and the nominal toughness is enhanced, even in the absence of friction.

3.3 Effects of modulus mismatch. When there is a modulus mismatch across the interface, such that $\beta \neq 0$, the phase angle, as defined by linear-elasticity depends on the length scale chosen to describe it (Rice, 1988). In particular, if the nominal phase angle is described by the laminate thickness, h_1, as indicated in Eqn. 11, then the phase angle can be shifted to a new reference scale, ξ, by

$$\psi = \psi^{\infty} + \epsilon \ln(\xi/h_1). \tag{15}$$

If $\Gamma_{II}/\Gamma_I = 1$, then the possible complications of a modulus mismatch are limited to frictional dissipation if the surfaces of the crack are forced into contact by the oscillatory displacement field. However, the general problem of mixed-mode fracture is complicated by a lack of knowledge about the appropriate length scale with which to define the phase

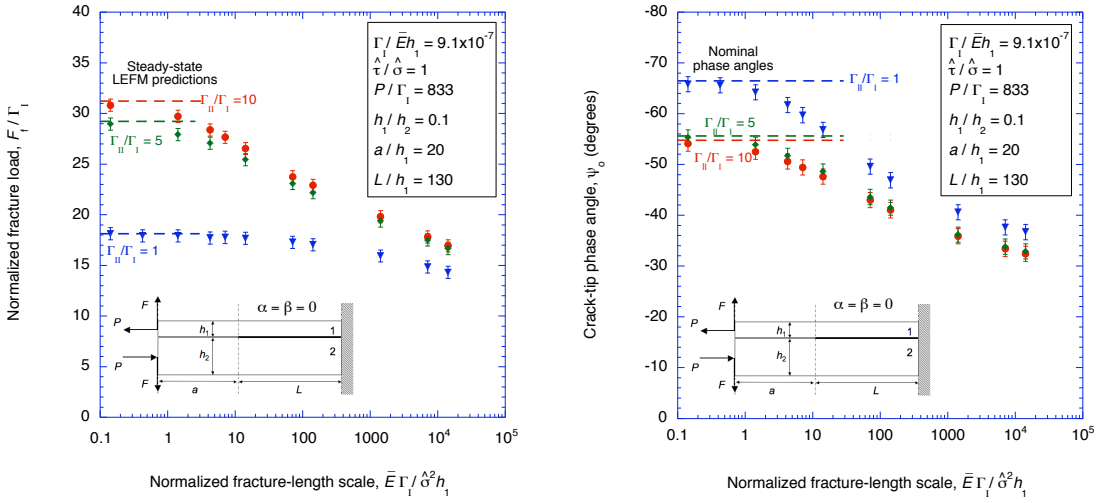

Fig. 13: **(a)** Variation of the strengths of a laminated geometry with the fracture length scale, and a comparison with the LEFM predictions for the strength. **(b)** Associated crack-tip phase angles. Figures adapted from Parmigiani and Thouless (2007).

angle. A cohesive-zone model incorporates a length scale naturally (Parmigiani and Thouless, 2007). As can be seen from Fig. 15a, the phase angle for a laminated geometry with a non-zero value of β plateaus at the crack tip, in the same way that the phase angle plateaus when $\beta = 0$. This crack tip value of ψ_o is the phase angle that controls fracture. It will be noted from Fig. 15a that the cohesive-zone parameters chosen for the plot are such that the fracture-length scale is sufficiently small for there to be a small region in which the phase angle has a logarithmic dependence on distance from the crack tip, as predicted by LEFM (Rice, 1988). Furthermore, a series of calculations using the same cohesive zone, but with different elastic mismatches indicates that the appropriate length scale to describe the phase angle in this particular case is $0.0018h_1$ (Fig. 15b). No obvious link has been found between this length scale and any features of the cohesive zone.

4. CRACK DEFLECTION INTO AN INTERFACE

As described in Section 2.1, an LEFM calculation of whether a crack will kink into an interface of a laminate (Fig. 16a) is done by comparing the energy-release rates for a small kink of length k extending across the interface with the energy-release rate for the separate problem of a small kink, also of length k, deflecting into the interface. If the modulus is the same on both sides of the interface, and $h_1 << h_2$, the condition for crack deflection is (He *et al.* 1994)

$$\Gamma_2/\Gamma \geq 3.83 + 5.77(k/h_1)^{1/2} + 2.18(k/h_1). \tag{16}$$

where Γ_2 is the mode-I toughness of the material beneath the interface, and Γ is the appropriate mode-dependent toughness of the interface (which depends on Γ_I and Γ_{II}). Cohesive-zone calculations for crack deflection introduce three additional parameters: the mode-I and mode-II cohesive strengths for the interface, $\hat{\sigma}$ and $\hat{\tau}$, and the mode-I cohesive strength for the substrate $\hat{\sigma}_2$. Cohesive-zone calculations for the two separate problems of deflection

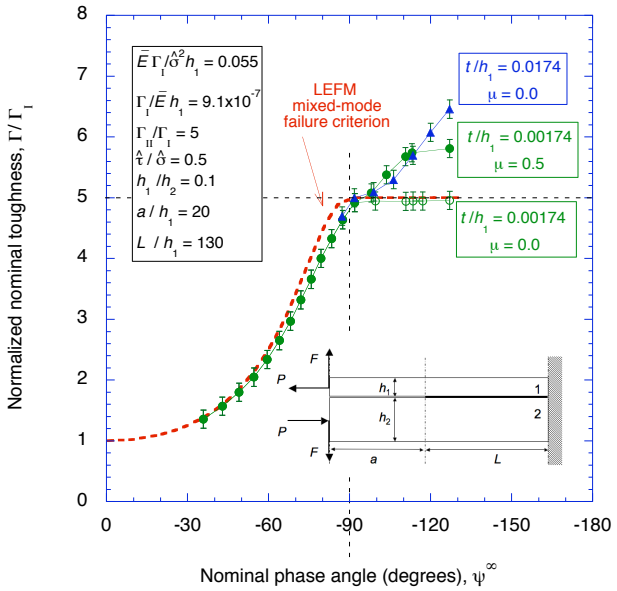

Fig. 14: Normalized nominal toughness as a function of nominal phase angle for a laminated geometry with different thicknesses of cohesive layer, and different coefficients of friction ($\mu = 0$ and $\mu = 0.5$). Modified figure from Parmigiani and Thouless (2007).

and propagation, with kink sizes much smaller than the relevant fracture-length scales of $\bar{E}\Gamma_I/\hat{\sigma}^2$ and $\bar{E}\Gamma_2/\hat{\sigma}_2^2$, result in excellent agreement with the expression given in Eqn. 16 (Parmigiani and Thouless, 2006).

However, significantly different results are obtained when cohesive elements are placed along the interface and through the substrate simultaneously (Fig. 16b). Under these conditions, the cohesive-zone calculations permit the crack to chose whether to propagate across the interface or to deflect along it, rather than being set *a priori*. The conditions for deflection or penetration in a homogeneous system with $\Gamma_{II}/\Gamma_I = 1$ are shown in Fig. 17a. This figure shows that crack deflection is promoted by high values of both $\hat{\sigma}_2/\hat{\sigma}$ and Γ_2/Γ_I. Conversely, crack penetration is promoted by low values of these two ratios. There appears to be a critical value of the strength ratio ($\hat{\sigma}_2/\hat{\sigma}$) below which crack penetration is guaranteed, irrespective of the toughness ratio. This limit was explored using fracture-length scales well into the regime where LEFM is expected to be valid, and was determined to be about 3.2 for elastically homogeneous laminates. This value is very consistent with the results of analyses based on strength criteria (Cook and Gordon 1964; Gupta, *et al.* 1992). In contrast to LEFM analyses, there does not appear to be a critical toughness ratio that ensures crack penetration.

Similar results were obtained from calculations with a modulus mismatch. While, in general, both the toughness and strength ratios determine whether crack deflection or penetration takes place, there appear to be lower bounds for $\hat{\sigma}_2/\hat{\sigma}$ below which crack penetration will always occur (Fig. 17b). Mode-II effects for the interfacial cohesive zone become particularly important when the crack resides in the stiffer material ($\bar{E}_1 > \bar{E}_2$). A relatively large value of mode-II interfacial toughness impedes delamination under these conditions, thus increasing the tendency for the crack to propagate through to the substrate. Conversely, when the substrate is stiff ($\bar{E}_1 < \bar{E}_2$), mixed-mode effects are less important, and the possibility of

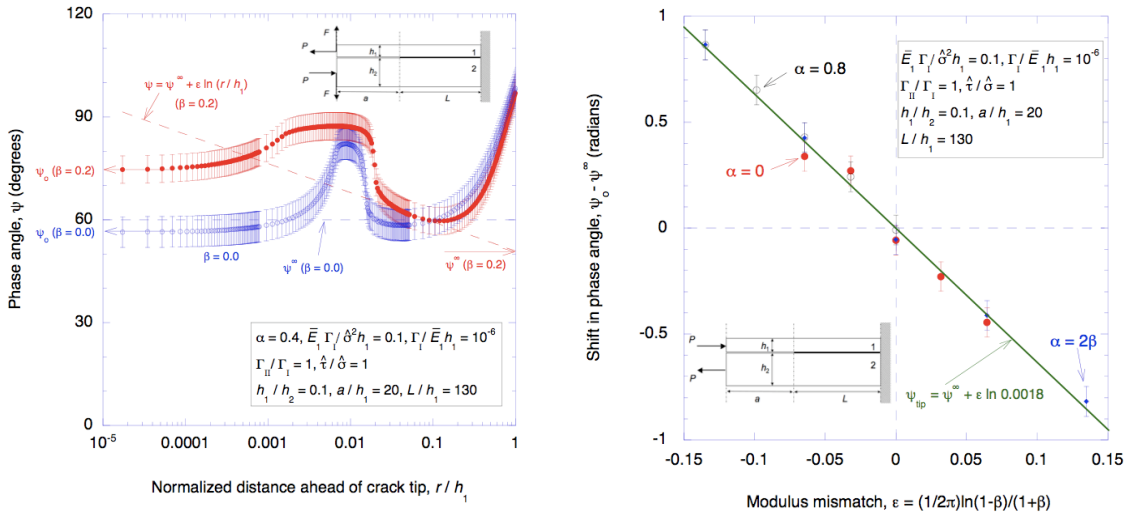

Fig. 15: **(a)** Phase angles for a mixed-mode geometry with a modulus mismatch. **(b)** Shift in phase angle between the crack tip phase angle and the nominal phase angle defined in terms of h_1 as a function of the mismatch parameter ϵ. This plot shows that the characteristic length scale describing fracture for this particular cohesive law is $0.0018h_1$. Figures taken from Parmigiani and Thouless (2007).

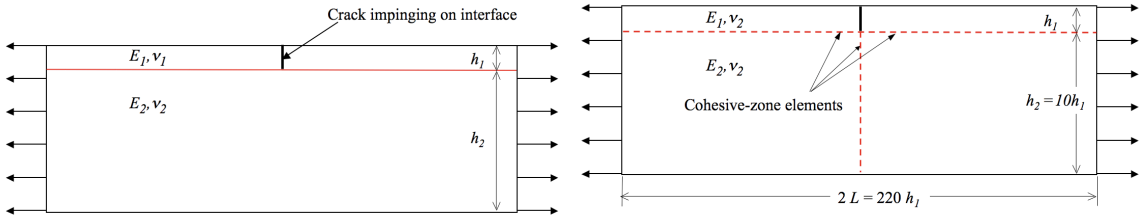

Fig. 16: **(a)** The geometry for crack deflection at an interface in a laminated geometry. **(b)** Geometry for a cohesive-zone model for crack deflection. Figures adapted from Parmigiani and Thouless (2006).

crack deflection is enhanced.

The apparent difference between the criteria for crack deflection from LEFM calculations and from cohesive-zone calculations can be rationalized examining the magnitude of the applied stress required to propagate the crack along the interface or into the substrate (Fig. 18). If $\Gamma_{II}/\Gamma_I = 1$, the applied stress required to propagate a kink across an interface of the elastically homogeneous laminate shown in Fig. 16a is

$$\sigma_a = 0.471\sqrt{\bar{E}_1\Gamma_2/h_1} \tag{17}$$

while the applied stress required to deflect the crack along the interface is

$$\sigma_a = 0.923\sqrt{\bar{E}_1\Gamma_I/h_1} \tag{18}$$

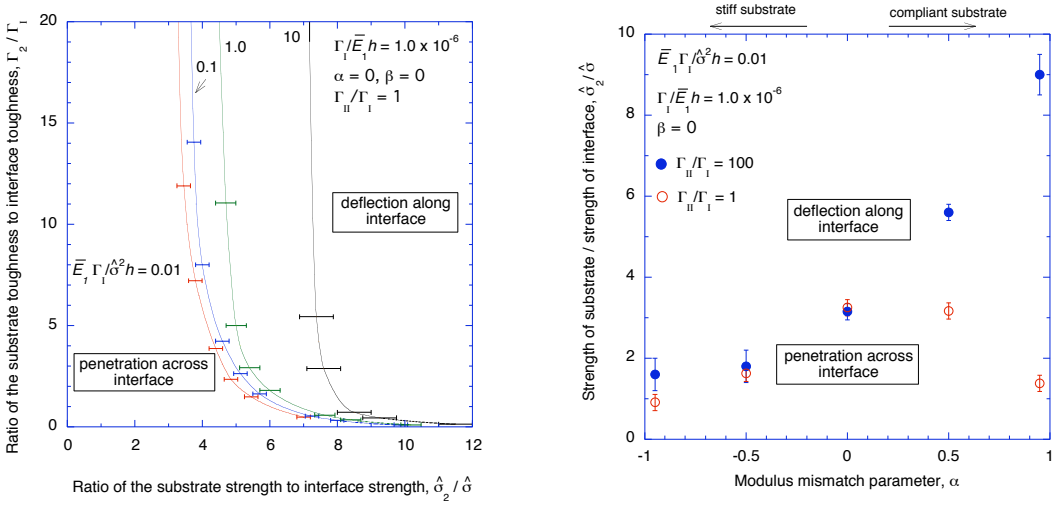

Fig. 17: **(a)** The conditions for a transition between crack deflection and propagation at an interface with no elastic mismatch. **(b)** The lower-bound for the strength ratio associated with the transition at an interface with elastic mismatch. Figures adapted from Parmigiani and Thouless (2006).

These equations have been plotted on Fig. 18, from which the LEFM result of $\Gamma_2/\Gamma_I = 3.83$ for the transition between deflection and penetration can be seen graphically. In the limits of very high and very low values of the ratio Γ_2/Γ_I, the cohesive-zone model agrees with the two LEFM results for the stresses required to deflect or propagate the crack. However, in general, the cohesive zones that develop in the substrate or along the interface shield each other, and raise the required stresses for both mechanisms. This interaction between the two cohesive zones is believed to be at the heart of the discrepancy between the LEFM results of He and Hutchinson (1989), and the cohesive-zone results presented above. When the fracture-length scales for the substrate and interface are comparable (or when the fracture-length scale of the substrate is larger than that of the interface), interfacial crack growth is shielded more strongly than crack penetration across the interface. This shifts the criterion for the transition to higher values of Γ_2/Γ_I (or, equivalently, to lower values of $\hat{\sigma}_2/\hat{\sigma}$). When the fracture-length scale for the substrate is significantly smaller than that for the interface, crack penetration across the interface is shielded more strongly than crack deflection. Under these conditions, the critical toughness ratio decreases, and the critical stress ratio increases.

An estimate of the amount of shielding provided by the cohesive zones, can be obtained by solving the LEFM problem for a crack impinging on an interface with *simultaneous* kinks extending across the interface and along the interface. This problem has been solved by finite-element methods. If the kinks are all of equal size ($k/h = 10^{-}5$), the applied stress required to propagate a kink across an interface in an elastically homogeneous laminate is

$$\sigma_a = 0.543\sqrt{\bar{E}_1\Gamma_2/h_1}. \tag{19}$$

This is not significantly different from the result of Eqn. 17. However, the stress required to propagate a kink along the interface is raised substantially by the presence of a substrate

kink to

$$\sigma_a = 1.699\sqrt{\bar{E}_1 \Gamma_I / h_1} \tag{20}$$

A comparison of these two equations indicates that a transition between the two modes of crack growth would occur at a toughness ratio of $\Gamma_2/\Gamma_I = 9.79$. It will be observed that this is very close to the critical ratio shown in Fig. 18a when the cohesive zones along the interface and in the substrate are comparable. Furthermore, it can be seen from Fig. 18 that the maximum stress, when the cohesive zone sizes are comparable, is almost identical to that given by Eqn. 20. It is expected that repeating similar LEFM calculations for different relative sizes of kinks would rationalize the range of deflection behavior observed in the cohesive-zone analyses for different fracture-length scales. The relative cohesive strengths affect the transitions between deflection and penetration behavior, even in the range of cohesive parameters where LEFM results are expected to be valid, because the relative strengths affect the relative lengths of the cohesive zones.

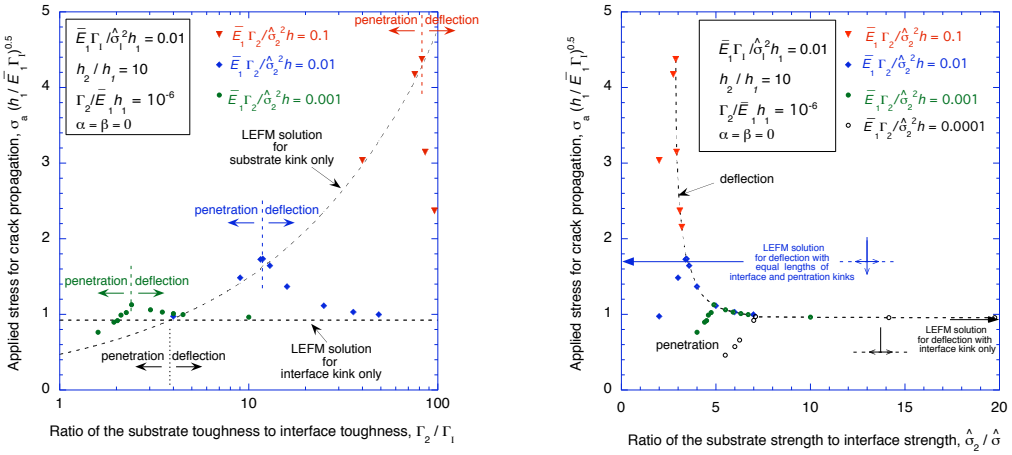

Fig. 18: The applied stress to propagate a crack, either along the interface or across it, for different fracture-length scales as a function of **(a)** toughness ratio, and **(b)** strength ratio.

5. CONCLUSIONS

Cohesive-zone models of fracture provide a natural bridge between conditions in which energy-based fracture criteria are appropriate and the conditions in which strength-based fracture criteria are appropriate. A mixed-mode cohesive-zone model has been used to explore the concepts of phase angle and mixed-mode failure criteria. It has been shown that linear-elastic fracture mechanics (LEFM) analyses of mixed-mode delamination are very robust, providing excellent predictions for the crack-tip phase angle and delamination strength, even under conditions which might not seem to be appropriate for using the equations of LEFM. In particular, the notion of a phase angle calculated from LEFM seems to be appropriate, even when the stress distribution along the interface has no relationship to what would be expected from a linear-elastic analysis. A finite thickness that can be associated with a cohesive zone, permits delamination to occur when the interface is subjected to a compressive stress. This provides an additional contribution to the energy

dissipation, beyond friction, that can raise the nominal toughness of an interface above the mode-II toughness. Since they involve a fracture-length scale, cohesive-zone models allow delamination in the presence of a modulus mismatch to be modelled naturally.

Crack deflection at interfaces can also be modelled by mixed-mode cohesive-zone models. It has been shown that the interaction between competing cohesive zones fundamentally changes the problem from existing LEFM models of crack deflection. In particular, the relative magnitudes of the cohesive strengths of the interface and substrate play an important role in determining the transition between crack deflection and penetration.

REFERENCES

Cook, J., and Gordon, J.E. (1964). A mechanism for the control of crack propagation in all-brittle systems. Proc. R. Soc. London, Ser. A282, 508-520.

Dundurs, J. (1969). Edge-bonded dissimilar orthogonal elastic wedges. J. App. Mechs. 36, 650-652.

Griffith, A.A., (1920). The phenomenon of rupture and flow in solids. Philos. Trans. Roy. Soc. London A221, 163-198.

Gupta, V., Argon, A.S., and Suo, Z. (1992). Crack deflection at an interface between two orthotropic media. J. Appl. Mechs. 59, S79-S87.

He, M. Y. and Hutchinson, J. W. (1989). Crack deflection at an interface between dissimilar elastic materials. Int. J. Solids Structures, 25, 1053-1067.

He, M. Y., Evans, A. G. and Hutchinson, J. W. (1994). Crack deflection at an interface between dissimilar elastic materials: Role of residual stresses. Int. J.Solids Structures 31, 3443-3455.

Hsueh, C. H. (1990). Interfacial debonding and fiber pull-out stresses of fiber-reinforced composites. Mat. Sci. Eng. A123, 1-11.

Inglis, C.E., (1913). Stresses in a plate due to the presence of cracks and sharp corners. In: Proceedings of the Institute of Naval Architects, vol. 55., pp. 219-230.

Li, S., Thouless, M. D., Waas, A. M., Schroeder, J. A., and Zavattieri, P. D. (2005a). Use of mode-I cohesive-zone models to describe the fracture of an adhesively-bonded polymer-matrix composite. J. Comp. Sci. Technol. 65, 281-293.

Li, S., Thouless, M. D., Waas, A. M., Schroeder, J. A., and Zavattieri, P. D. (2005b). Use of a cohesive-zone model to analyze the fracture of a fiber-reinforced polymer-matrix composite. J. Comp. Sci. Technol. 65, 537-549.

Li, S., Wang, J., and Thouless, M. D. (2004). The effects of shear on delamination in layered materials. J. Mech. Phys. Solids, 52,193-214.

Li, V. C., Maalej, M., and Hashida,T. (1994). Experimental determination of the stress-crack opening relation in fibre cementitious composites with a crack-tip singularity, J. Mat. Sci. 29, 2719-2724.

Marshall, D. B., Cox, B. N., and Evans, A. G. (1985). The mechanics of matrix cracking in brittle matrix composites, Acta Metall. 33, 2013-2021.

Muki, R. and Sternberg, E. (1970). Elastostatic load-transfer to a half-space from a partially embedded axially loaded rod. Int. J. Solids Structures 6, 69-90.

Parmigiani, J. P., and Thouless, M. D. (2006). Roles of toughness and cohesive strength on crack deflection. J. Mech. Physics Solids 54, 266-287.

Parmigiani, J. P., and Thouless, M. D. (2007). The effects of cohesive strength and toughness on mixed-mode delamination of beam-like geometries. Eng. Frac. Mechs. (in press).

Rice, J. R. (1988). Elastic fracture-mechanics concepts for interfacial cracks. J. App. Mechs. 55, 98-103.

Sørensen B. F. and Jacobsen, T. K. (2003). Determination of cohesive laws by the J-integral approach. Eng. Frac. Mechs. 70, 1841-1858.

Stringfellow, R. G., and Freund, L. B. (1993). The effect of interfacial friction on the buckle-driven spontaneous delamination of a compressed thin film. Int. J. Solids Stuctures 30, 1379-1395.

Suo, Z., and Hutchinson, J. W. (1990). Interface crack between two elastic layers. Int. J. Fract. 43, 1-18.

Thouless, M. D., Cao, H. C. and Mataga, P. A. (1989). Delamination from surface cracks in composite materials. J. Mat. Sci. 24, 1406-1412.

Thouless, M. D., Hutchinson,J. W. and Liniger, E. G. (1992). Plane strain buckling-driven delamination of thin films: Model experiments and mode-II fracture. Acta Metall. Mater. 40, 2639-2649.

Thouless, M. D., Jensen, H. M. and Liniger, E. G. (1994) Delamination from edge flaws. Proc. Roy. Soc. A447, 271-279.

Yang, Q. D., Thouless, M. D., and Ward, S. M. (1999). Numerical simulations of adhesively-bonded beams failing with extensive plastic deformation. J. Mech. Phys. Solids, 47, 1337-1353.

Yang, Q. D., and Thouless, M. D. (2001). Mixed-mode fracture analyses of plastically-deforming adhesive joints. Int. J. Fract. 110, 175-187.